Childs Nerv Syst (2014) 30:1333–1342
DOI 10.1007/s00381-014-2446-z

ORIGINAL PAPER

Traumatic brain injury alters long-term hippocampal neuron morphology in juvenile, but not immature, rats

Eric M. Casella · Theresa Currier Thomas · Dana L. Vanino · Wendy Fellows-Mayle · Jonathan Lifshitz · J. Patrick Card · P. David Adelson

Received: 31 January 2014 / Accepted: 19 May 2014 / Published online: 1 June 2014

Abstract
Purpose Pediatric traumatic brain injury (TBI) represents a prominent yet understudied medical condition that can profoundly impact brain development. As the juvenile injured brain matures in the wake of neuropathological cascades during potentially critical periods, circuit alterations may explain neurological consequences, including cognitive deficits. We hypothesize that experimental brain injury in juvenile rats, with behavioral deficits that resolve, will lead to quantifiable structural changes in hippocampal neurons at chronic time points post-injury.
Methods Controlled cortical impact (CCI), a model of focal TBI with contusion, was used to induce brain injury on postnatal day (PND) 17 juvenile rats. The histological consequence of TBI was quantified in regions of the hippocampus at post-injury day 28 (PID28) on sections stained using a variation of the Golgi-Cox staining method. Individual neuronal morphologies were digitized from the dentate gyrus (DG), CA3, and CA1 regions.
Results Soma area in the ipsilateral injured DG and CA3 regions of the hippocampus increased significantly at PID28 in comparison to controls. In CA1, dendritic length and dendritic branching decreased significantly in comparison to controls and the contralateral hemisphere, without change in soma area. To extend the study, we examined neuronal morphology in rats with CCI at PND7. On PID28 after CCI on PND7 rats, CA1 neurons showed no injury-induced change in morphology, potentially indicating an age-dependent morphological response to injury.
Conclusions Long-lasting structural alterations in hippocampal neurons of brain-injured PND17 juvenile animals, but not PND7 immature animals, suggest differential plasticity depending on age-at-injury, with potential consequences for later function.

Keywords Golgi · Juvenile traumatic brain injury (TBI) · Controlled cortical impact injury (CCI) · Rats · Hippocampus · Dendritic length · Branching points · Soma area

Eric Casella and Theresa Currier Thomas contributed equally to this paper

E. M. Casella · T. C. Thomas · J. Lifshitz · P. D. Adelson (✉)
Barrow Neurological Institute, Phoenix Children's Hospital, Ambulatory Building B, 4th Floor, 1919 East Thomas Road, Phoenix, AZ 85016, USA
e-mail: dadelson@phoenixchildrens.com

E. M. Casella · T. C. Thomas · J. Lifshitz · P. D. Adelson
Department of Child Health, University of Arizona College of Medicine–Phoenix, Phoenix, AZ 85004, USA

T. C. Thomas · J. Lifshitz
Phoenix VA Healthcare System, Phoenix, AZ 85012, USA

J. Lifshitz · P. D. Adelson
Neuroscience Program, Arizona State University, Tempe, AZ 85287, USA

P. D. Adelson
School of Biological and Health Systems Engineering, Arizona State University, Tempe, AZ 85287, USA

J. P. Card
Department of Neuroscience, University of Pittsburgh, Pittsburgh, PA 15260, USA

W. Fellows-Mayle
Department of Neurological Surgery, University of Pittsburgh, Pittsburgh, PA 15213, USA

D. L. Vanino
Medical University of South Carolina, Charleston, SC 29412, USA

Introduction

Head trauma remains a significant pediatric health problem, with an estimated incidence of 230/100,000 leading to

100,000–200,000 new pediatric traumatic brain injuries (TBI) each year, of which children 0–4 have the highest rates of TBI-related emergency room visits, hospitalizations, and deaths [1–5]. Approximately 10–15 % of childhood TBI is severe and leading to death or permanent brain damage [6, 7]. Significant motor and cognitive deficits can occur after mild to moderate TBI [8–11]. In fact, children less than 4 years old have a worse outcome in comparison to older children and adults [10, 12]. Hence, juvenile TBI burdens both families and society with health care and associated costs [5], for which outcome depends on age-at-injury and necessitates translational relevant knowledge to minimize adverse consequences of injury.

Controlled cortical impact (CCI) is an experimental model of TBI that is clinically relevant to brain injuries resulting in contusion. Primarily a focal cortical injury depending on depth of penetration, CCI allows for control over mechanical parameters (velocity, depth of impact), has been well studied, [13–20], and results in reproducible behavioral deficits in the developing, immature rat [21]. For developing animals, protocols from the adult have been adapted and scaled to study injury-induced pathology and behavioral deficits [21, 22]. Post-natal rats mature rapidly, such that by 28 days post-injury, they have reached adolescence or young adulthood. Unilateral CCI in the juvenile rodent permits histological analysis of both neuronal morphology in proximity (ipsilateral) and distal (contralateral) to the site of contusive injury.

Over 28 days after CCI in juvenile rodents, both transient and long-lasting behavioral deficits have been associated with cortical and hippocampal pathology. Rats receiving a 2.0-mm deflection CCI on post-natal day (PND) 17 showed significant memory and learning deficits in the Morris Water Maze paradigm beginning at post-injury day (PID) 11 and lasting until at least PID17 in comparison to uninjured sham rats [21]. In comparable studies using similar injury parameters, cognitive deficits resolved by PID28 [21, 23, 24]. However, somatic and emotional dysfunction, measured by sensorimotor function and anxiety-like behaviors, persist through PID60 after experimental TBI at PND17 in the absence of spatial learning and memory deficits [24]. Performance in these tasks depends on hippocampal function, suggesting that circuit reorganization and underlying changes in neuron morphology may mediate the transient deficits and long-lasting deficits.

Long-lasting changes in neuronal structure occur after CCI in PND17 rats, where a greater number of neurons have incorporated into hippocampal circuitry at PID28 [25]. Injury-induced damage that extends into white matter tracts at PID60 suggests that TBI at a young age can cause long-term connectivity changes alongside persisting behavioral deficits [24]. In impact-acceleration TBI at PND17, cognitive dysfunction endures through 3 months post-injury [26], despite no obvious neuronal loss [27]. Although injury-induced alterations in circuit structure have been implicated in both transient and long-lasting behavioral deficits, cytoarchitectural changes have not been evaluated at the level of individual neurons. In addition, the developmental period at the time of injury impacts outcome. PND17 is likely beyond the most vulnerable developmental period, but histopathological analysis of the immature brain after impact-acceleration brain trauma revealed peak apoptotic cell death up to PND14, and vulnerability rapidly decreased thereafter [28, 29]. Thus, age-at-injury may influence outcome in regard to neuronal circuitry, with consequences for functional outcome.

In the present study, we sought to further quantify the morphological changes that occur concurrent with development and reorganization of the hippocampus at 28 days post-injury, building on our previous studies [21, 25, 30]. Our goal is to regionally define morphological changes in hippocampal neurons to attribute circuit alterations to the nature of cognitive deficits previously reported [21]. The Golgi method is ideally suited for defining trauma-induced pathology because it reveals the details of cellular morphology that cannot be readily assessed with other histological methods. The extent of these changes will be measured by analyzing soma area, dendritic length, and dendritic branching. We hypothesize that CCI in the juvenile rat will lead to chronic quantifiable structural changes in neurons of hippocampal subregions. Furthermore, there will be injury-induced changes in morphology in younger (PND7) animals that will differ from PND17.

Methods

Experimental groups

Adult female Sprague-Dawley rats with timed pregnancy (Harlan Sprague-Dawley; Indianapolis, IN) were used with each litter culled to eight male pups. At PND17, the rat pups from the same litter were randomly assigned to one of three groups: trauma (n=4), sham (n=2), and naïve (n=2). A second litter at PND7 was assigned to one of two groups: trauma (n=6) and sham (n=2). The dams and their litters pre- and post-injury all followed the same protocol and were maintained in standardized conditions throughout the study (12-h light/dark cycle with lights on at 0700; 22 °C). Food and water were available ad libitum. These experiments were approved by the University of Pittsburgh Institutional Animal Care and Use Committee (protocol #0009975).

Surgical preparation

The surgery and injury have previously been described [21]. Briefly, on PND17 (or PND7), rat pups were initially anesthetized with 1.5–2.0 % isoflurane in N_2O/O_2 (2:1) using a nose cone; core temperature was maintained at 37.0–37.5 °C

throughout the procedure by a heating pad and monitored by rectal thermometer. The scalp was shaved and sterilely prepared. The head was secured in a stereotaxic head frame and the skull exposed by a midsagittal incision and reflection of the scalp. Using a high-speed air drill, a craniotomy (7.0 mm for PND17; 4.0 mm for PND7) was made in the left parietal bone at 0.2 mm posterior to the coronal suture and 0.2 mm anterior to lambdoid suture, extending laterally to the superior temporal line.

Controlled cortical impact

Controlled cortical impact (CCI) was performed to induce severe traumatic brain injury, as described [21, 25, 31]. Briefly, the dura mater was exposed by removing the bone flap, and the piston of the CCI was positioned to deliver a focal cortical impact. Anesthesia was discontinued until the toe pinch reflex returned. The impact was delivered with a 6-mm or 3-mm tip (PND17 or 7, respectively) at a controlled velocity of 4 m/s over 500 ms. The piston was calibrated to produce an injury deflection depth of 2.0 mm for PND17 animals. In PND7, the injury depth was reduced to 1.75 mm to account for the smaller size of the animals, as previously described [21]. Sham controls were subjected to the same surgical procedures with no impact. Naïve animals had neither surgery nor injury. Immediately following injury, anesthesia was resumed, the bone flap replaced and secured with Koldmount dental cement (Vernon-Benshoff, Albany, NY), and the scalp incision sutured. The rats were transferred to a warmed recovery cage and observed for at least 30 min. After resumption of normal gait (~30 min), the rat pups were returned to their litters and observed intermittently over the next 30 min to ensure acceptance by their dams.

Golgi-Cox procedure

On post-injury day 28 (PID28), all animals were anesthetized and perfused transcardially with a 10 % formalin solution using a peristaltic pump. Each brain was removed, blocked in 6-mm coronal sections, and post-fixed for 3 days at room temperature. Using a modification of the Golgi-Cox procedure that produces extensive and reproducible impregnation of neurons, the tissue sections were transferred to a Golgi-Cox solution that consists of 20 parts 5 % potassium dichromate, 20 parts 5 % mercuric chloride, 8 parts 5 % potassium chromate, and 40 parts distilled water. The tissue was kept in solution in the dark at room temperature for 2 months, with a transfer to a fresh solution each week [32, 33]. This period of incubation was optimized to maximize the silver impregnation of the neurons and their branches and dendritic arbors while minimizing impregnation of overlapping neurons. After this incubation period, the tissue blocks were sectioned serially through the rostrocaudal extent of the injury in the coronal plane using a vibratome at 200 μm and collected sequentially in 0.1 M sodium phosphate buffer. Thereafter, sections were dehydrated in a graded ethanol series (50, 70, 95, 100 %), cleared in clove oil, infiltrated in Cytoseal 60 (VWR Scientific), and coverslipped on gelatin-coated slides using Cytoseal 60.

Data collection/analysis

Data collected from the injured hippocampus were compared to homotypic regions of the contralateral uninjured hemisphere and from equivalent regions of controls (sham and naïve animals for PND17). Using Neurolucida software (MicroBrightField, Inc., Colchester, VT), the location of all impregnated perikarya was mapped for granule cells of the DG and pyramidal cells of area CA3 and area CA1. Neurons were selected for reconstruction based on the presence of an intact soma, the absence of truncations of large dendrites, and presence of natural ends. A natural end was defined as the termination of a completely tapered dendrite, identifiable by the presence of an end swelling, spine or spine cluster, or gradual narrowing. 3D reconstruction of neuron morphology was carried out by an investigator blinded to injury status using Neurolucida. The boundaries of the soma of each neuron were traced using a ×60 objective, and the predicted contour of the cell soma was followed. Then, all dendrites emerging from the cell soma were traced through their full extent. The completed reconstructions were analyzed using the NeuroExplorer program (MicroBrightField, Inc., Colchester, VT) to calculate soma area, dendritic length, and branch points. The linear extent of all components of the dendritic arbor and the number of branch points were summed. The same measures from equivalent populations of neurons from the uninjured hemisphere and sham/naïve animals served as the control population. Approximately 90 neurons in each hemisphere per animal were digitized from the dentate gyrus, 20 neurons in each hemisphere per animal in the CA3 region, and 60 neurons in each hemisphere per animal in the CA1 region. In each control animal, neurons from both hemispheres were combined for approximately 150–180 neurons in the dentate gyrus, 40 neurons in the CA3 region, and 120 neurons in the CA1 region. The methods of data collection and analysis were identical for PND7 animals, with the focus only on the CA1 region.

Statistics

In PND17 animals, the average soma area, branch length, and branch points in neurons were compared. Sample size was based on preliminary data from the DG, CA3, and CA1, which indicated a group size of three to six animals were required to have 80 % power to detect a 10 % change from contralateral hemisphere with a statistical level of 0.05. Averages in PND17 naïve and sham animals were combined to create a single control group (n=4). Each quantitative measure

was subjected to statistical analysis by one-way ANOVA (GraphPad Prism 6). Neuron averages in each region of each animal were averaged for statistical analysis. Planned post hoc comparisons compared groups to identify significant differences between groups at the $p<0.05$ level.

In PND7 animals, where six animals were injured and two were shams, statistical analysis by *t* test was only performed on the six injured animals, comparing ipsilateral to contralateral measurements. Data from sham animals are included in the graphs, but not the statistical analysis. No statistical comparisons were conducted between PND17 and PND7 data.

Results

Soma area increased in the dentate gyrus 28 days following CCI injury

The soma area, cumulative dendritic length, and cumulative branch points of neurons in the DG were compared to the contralateral hemisphere and control animals in order to assess the impact of a severe CCI injury on neuron morphology at PID28 (Fig. 1). Soma area significantly increased in the ipsilateral hemisphere by 7.8 % in comparison to control animals ($F(2,9)=7.183$; $p=0.01$; Fig. 1c). The average soma area was

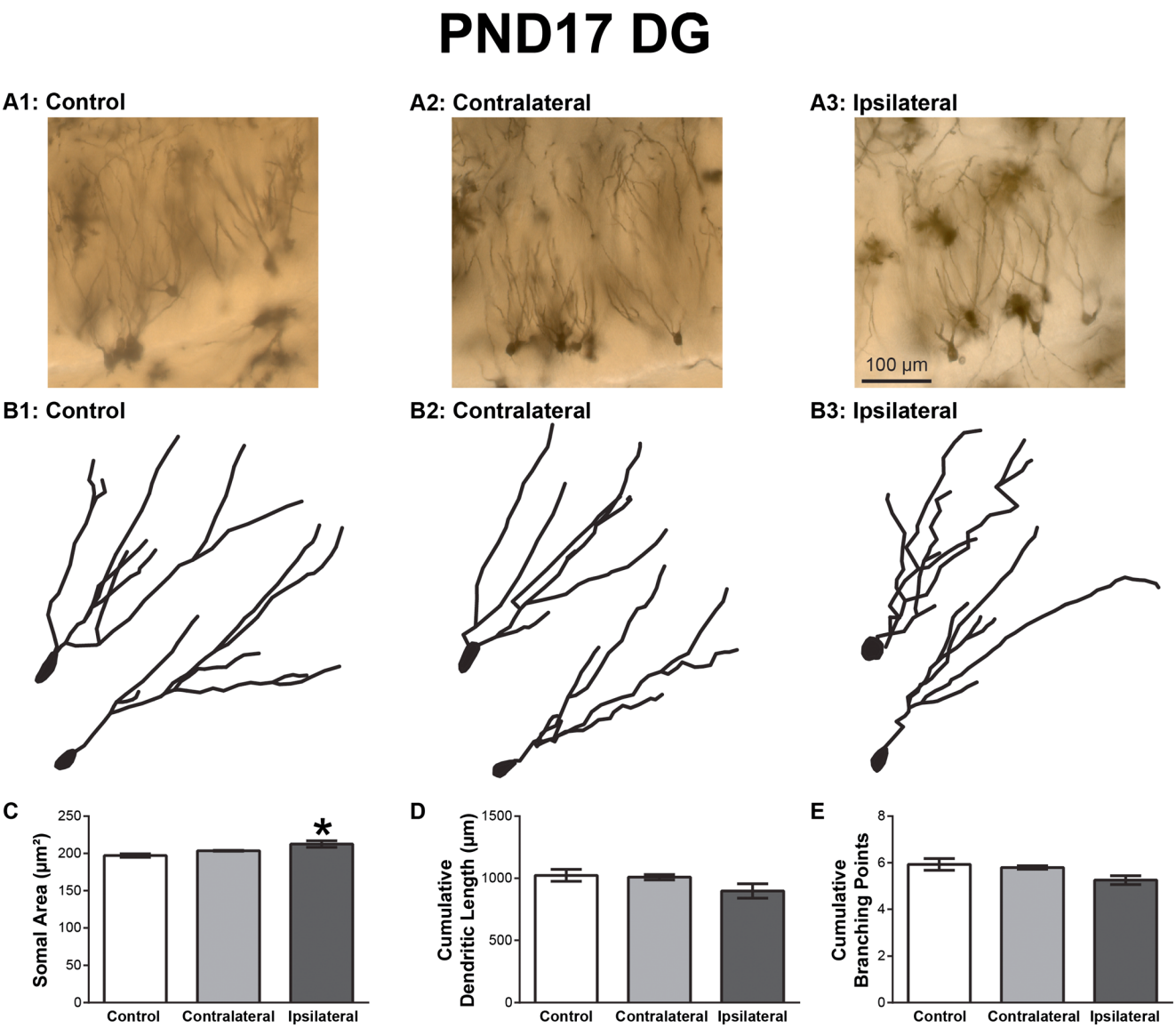

Fig. 1 For the dentate gyrus of the hippocampus, soma area significantly increased in the ipsilateral hemisphere of PND17 rats at 28 days after CCI compared to control (C). (A) Bright field images of Golgi stained dentate gyrus neurons from control (A1), contralateral hemisphere (A2) and ipsilateral hemisphere (A3) at PID28. (B) Representative neuron reconstructions from each location traced with the Neurolucida program. (D, E) No significant differences were measured in dendritic length or branching points between groups. Controls are the average of uninjured sham ($n=2$) and naïve ($n=2$) animals. Data were analyzed by one-way ANOVA with Tukey's post hoc comparison. Significance, *$p<0.05$ compared to controls. *Bar graphs* represent the mean±SEM with four animals per group. Magnification ×20

197.2±2.3 μm^2 in controls, 203.7±0.6 μm^2 in the contralateral hemisphere, and 212.6±4.4 μm^2 in the ipsilateral hemisphere. No significant changes in morphology were detected in dendritic length ($F(2,9)=2.293$; $p=0.16$; Fig. 1d) or number of branch points ($F(2,9)=3.622$; $p=0.07$; Fig. 1e). The average dendritic length ranged from 758 to 1,119 μm and average branch points ranged from 4.8 to 6.5 per neuron across all groups. These data indicate that soma area increased slightly in the ipsilateral DG, without change in dendritic architecture at 28 days after CCI compared to uninjured controls.

It is important to note that our preliminary observations indicated differences between the ventral and dorsal blade of the DG, with the dorsal blade more labile to morphological change after injury as measured by larger soma and shorter dendritic arborization [34]. This distinction was not borne out in the complete dataset; therefore, DG neurons from the ventral and dorsal blade have been pooled for analysis.

Soma area increased in the CA3 at 28 days following CCI injury

Morphological parameters of neurons in the CA3 were compared to the contralateral hemisphere and control animals in order to assess the impact of a severe CCI injury in PND17 animals on neuron morphology in the CA3 at 28 days post-injury (Fig. 2). Soma area significantly increased in the ipsilateral hemisphere by 11.3 % in comparison to control animals ($F(2,9)=4.657$; $p=0.04$; Fig. 2c). The average soma area was 401.8±5.5 μm^2 in controls, 414.7±15.6 μm^2 in the contralateral hemisphere, and 447.2±8.9 μm^2 in the ipsilateral hemisphere. No significant changes in morphology were detected in dendritic length ($F(2,9)=0.225$; $p=0.80$; Fig. 2d) or number of branch points ($F(2,9)=0.7594$; $p=0.4957$; Fig. 2e). The average dendritic length ranged from 1,693 to 3,088 μm and average branch points ranged from 13.6 to 24.1 per neuron across all groups. As in the DG, these data indicate that severe CCI injury resulted in an increased soma area in the ipsilateral CA3 at 28 days post-injury compared to uninjured controls.

Cumulative dendritic length and branching points decreased in the CA1 28 days following CCI injury

Morphological parameters of neurons in the ipsilateral brain-injured CA1 were compared to the contralateral hemisphere and control animals in order to assess the impact of a CCI injury in PND17 animals at 28 days post-injury (Fig. 3). No significant changes in soma area were detected ($F(2,9)=0.58$; $p=0.58$; Fig. 3c). The average soma area ranged from 287.2 to 301.2 μm^2 per neuron across all groups.

Dendritic length significantly decreased in the ipsilateral hemisphere by 20–26 % in comparison to controls and the contralateral hemisphere, respectively ($F(2,9)=13.36$; $p=0.002$; Fig. 3d). The average dendritic length was 2,564±85.9 μm in controls, 2,369±63.0 μm in the contralateral hemisphere, and 1,888±125.7 μm in the ipsilateral hemisphere.

The number of branching points significantly decreased in the ipsilateral hemisphere by 26.7 % in comparison to control animals and by 15.5 % in comparison to the contralateral hemisphere ($F(2,9)=32.98$; $p<0.0001$; Fig. 3e). In the contralateral hemisphere, there was a 13.3 % reduction in the number of branch points in comparison to control animals. The average cumulative branching points were 22.6±0.5 in controls, 19.6±0.4 in the contralateral hemisphere, and 16.6±0.5 in the ipsilateral hemisphere.

These data indicate that dendritic length and number of branching points in the ipsilateral hemisphere of the CA1 are susceptible to severe CCI at 28 days post-injury, without change in soma area.

No significant morphological changes in CA1 region of PND7 animals

The soma area, cumulative dendritic length, and cumulative branch points of neurons in the CA1 of PND7 animals were compared to the contralateral hemisphere in order to assess the impact of a severe CCI injury on morphology in the CA1 at 28 days post-injury (Fig. 4). No significant changes in morphology were detected in soma area between the ipsilateral and contralateral hemispheres ($F(2,11)=1.406$; $p=0.29$; Fig. 4a), with an average area ranging from 310.1 to 311.4 μm^2 per neuron across both groups (Fig. 4). No significant changes were detected for cumulative dendritic length ($F(2,11)=1.44$; $p=0.28$; Fig. 4b) or cumulative branching points ($F(2,11)=2.03$; $p=0.18$; Fig. 4c). The average cumulative dendritic length and branch points ranged from 2,195 to 2,546 μm per neuron and 19.3 to 22.8 per neuron across both groups, respectively. Calculations for sham animals were included in the figure, but not used for statistical analysis.

Discussion

In this study, we have shown that experimental TBI using CCI on PND17 rats results in increased soma area in the DG (7.8 %) and CA3 (11.3 %) regions of the hippocampus at PID28 in comparison to controls. Additionally, there was a 20–26 % injury-induced reduction in dendritic length and dendritic branching in the CA1 region in comparison to both the contralateral hemisphere and to controls. In younger PND7 rats, none of these morphological changes were observed in CA1, indicating an age-at-injury dependence on this morphological response to injury. These data indicate long-lasting morphological alterations of neurons in the

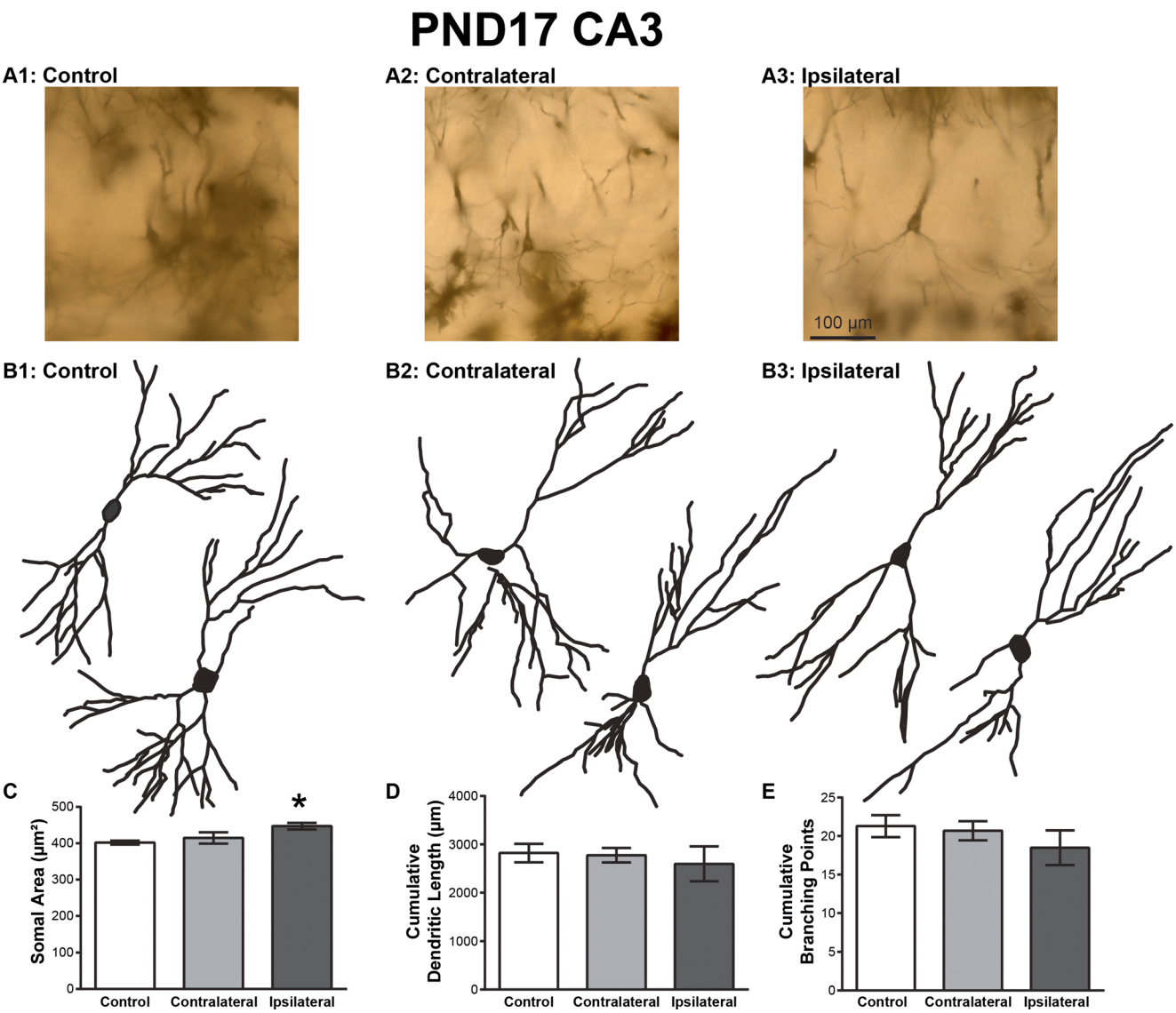

Fig. 2 For the CA3 of the hippocampus, soma area significantly increased in the ipsilateral hemisphere of PND17 rats at 28 days after CCI compared to control (C). (A) Bright field images of Golgi stained dentate gyrus neurons from control (A1), contralateral hemisphere (A2) and ipsilateral hemisphere (A3) at PID28. (B) Representative neuron reconstructions from each location traced with the Neurolucida program. (D, E) No significant differences were measured in dendritic length or branching points between groups. Controls (N=4) are represented by uninjured sham (n=2) and naïve (n=2) animals. Data were analyzed by one-way ANOVA with Tukey's post-hoc comparison. Significance, *p<0.05 compared to controls. *Bar graphs* represent the mean±SEM of four animals per group. Magnification ×20

hippocampus resulting from injury at PND17 that could impact continued brain development and influence the progression of post-injury cognitive function.

The increase in cell body size in the DG and CA3 may be interpreted as neuronal hypertrophy or selective loss of small neurons in these regions [35]. Hypertrophy is often considered a pathological event; however, insufficient evidence exists to correlate soma size to disease state [36]. Neuron hypertrophy can also result from increased metabolic or transcriptional demands, perhaps as compensation for neuron cell loss or accommodation of more neurons within the hippocampal trisynaptic pathway and subsequent synaptogenesis, as we previously reported in PND17 rats at PID28 [25, 35]. The absence of change in dendritic length and branch points in these regions is antithetical to the correlation between soma size and extent of dendritic arborization [35]. However, the neuronal and synaptic response to injury concomitant with developmental processes could negate this relationship. Assessment of neuron pathology and morphology at later-time points may reveal a role for hypertrophied soma in hippocampal circuit function in contrast to CA1.

To date, Nissl stains have been the principal means to define neuronal loss and contusion volume in experimental TBI. Yet, the Nissl selectively stains the endoplasmic

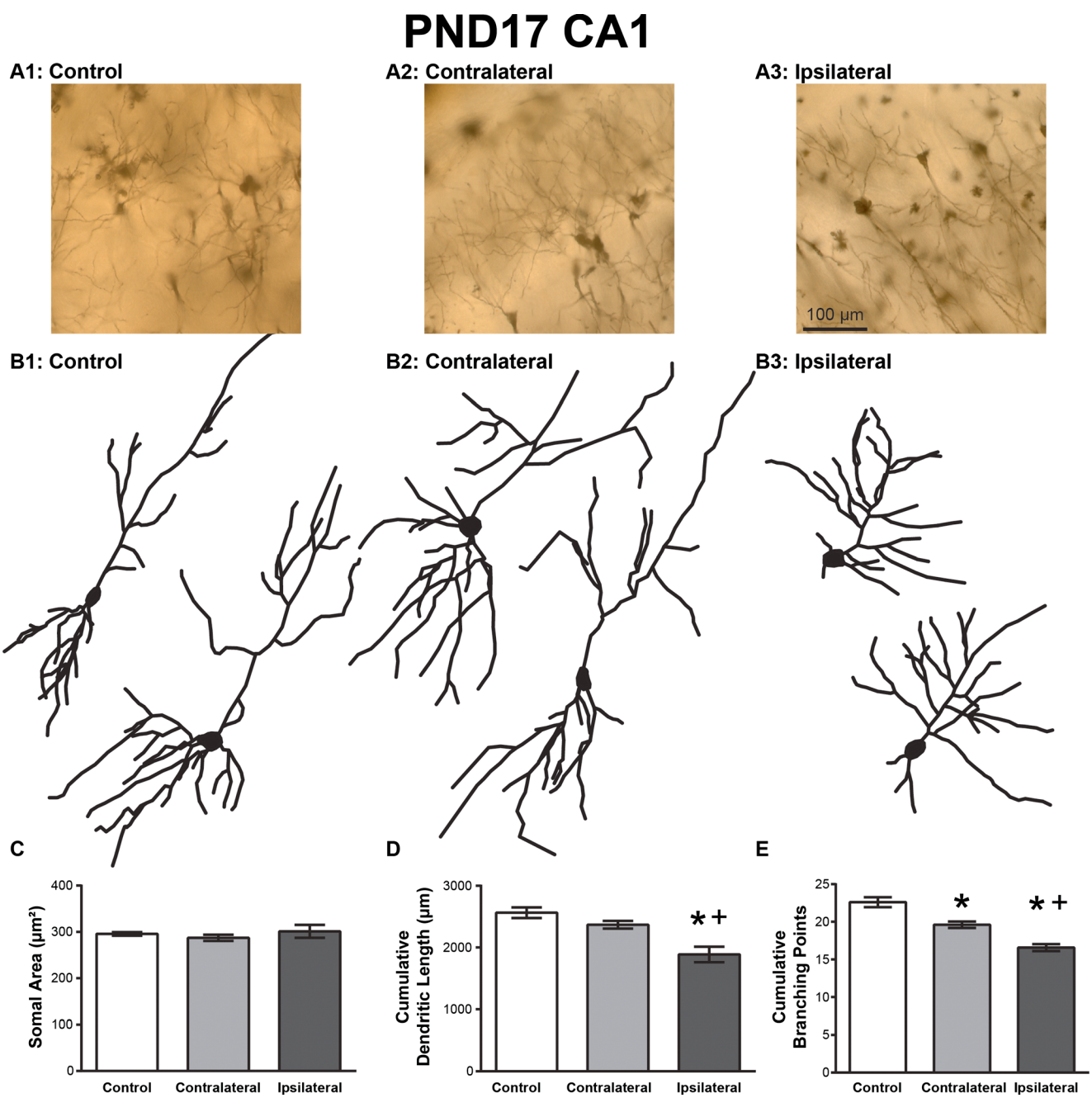

Fig. 3 For the CA1 of the hippocampus, dendritic length (D) and branching points (E) were significantly reduced in the ipsilateral hemisphere of PND17 rats at 28 days after CCI compared to control and the contralateral hemisphere. Significantly fewer branching points were also measured in the contralateral hemisphere compared to control (E). (A) Bright field images of Golgi stained CA1 neurons from control (A1), contralateral hemisphere (A2) and ipsilateral hemisphere (A3) at PID28. (B) Representative neuron reconstructions from each location traced with the Neurolucida program. (C) Soma area was not significantly different between groups. Data were analyzed by one-way ANOVA with Tukey's post hoc comparison. Significance, *$p<0.05$ compared to controls and + $p<0.05$ compared to contralateral hemisphere. *Bar graphs* represent the mean±SEM of four animals per group. Magnification ×20

reticulum and Nissl substance of the perikarya, while leaving neuronal processes essentially unstained. The Golgi stain can be used to visualize and characterize the morphology of the dendritic arbors, whose structure (branch length and branch points) directly reflects the magnitude of afferent input. The fine discrimination of individual neurons may better represent trauma-induced alterations in neuronal morphology, particularly as it relates to circuit function and behavioral performance.

Mechanical forces of injury induce differential strains on the CA1 and CA3 during CCI, which may explain the regional differences in morphology. Tensile strains are applied over a

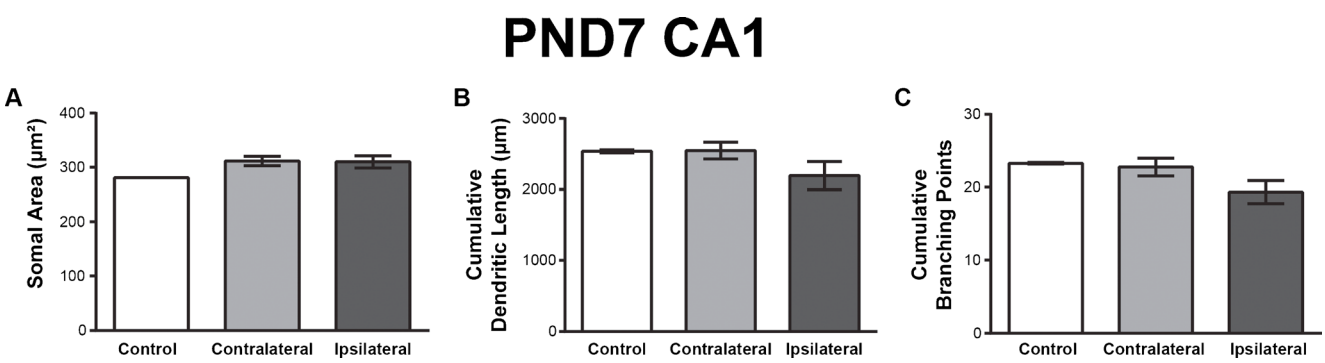

Fig. 4 CCI in PND7 rats did not cause significant change to the (**a**) soma area, (**b**) dendritic length, and (**c**) branching points at 28 days post-injury in the CA1 region of the hippocampus in comparison to the contralateral hemisphere. Sham (n=2); contralateral (n=6); ipsilateral (n=6). These data were analyzed with a one-way ANOVA with Tukey's post-hoc comparison. *Bar graphs* represent the mean±SEM. Magnification ×20

larger area and to a greater magnitude in the CA3 compared to CA1, indicating that CA3 may be more vulnerable to injury-inducing forces despite CA3 lying farther from the site of impact [37]. Additionally, significant CA3 neuronal loss has been repeatedly demonstrated after CCI [38–42], yet the extent of dendritic damage to either region has not been addressed, particularly in the juvenile animal. With the proximity of CA1 to the site of impact and the reduced incidence of cell death, it is plausible that CA1 neurons may preferentially sustain dendritic damage without cell death. Moreover, cell loss from the CA3 would result in afferent loss in the CA1, thereby influencing the extent of CA1 dendritic arborization [41].

Previously, we studied circuit reorganization in the hippocampus at PID28 following CCI in PND17 rats using viral transneuronal tracing [25]. This study demonstrated that more neurons were incorporated into hippocampal circuitry of the injured hemisphere compared to that of sham-operated controls. Injury-induced sprouting may expand the terminal arbors of neurons, ultimately incorporating more neurons into topographically organized circuits. Alternatively, neurons culled from the circuit by cell death could be compensated for in the normal course of development. In either condition, it is important to note that cognitive performance of injured animals in the Morris Water Maze returned to sham levels at the time that the synaptology of the circuit was analyzed (PID28) despite CCI-injured PND7 and PND17 rats displaying significant cognitive deficits at PID11–17 in comparison to sham rats [21, 25]. In diffuse TBI by impact acceleration in the juvenile, the extent of hippocampal reorganization, particularly as it relates to enduring cognitive deficits, is unknown [26, 27]. Thus, the injured developing brain may have the capacity to reorganize in a manner consistent with functional recovery.

Multiple laboratories have demonstrated that early cognitive deficits following CCI return to sham levels by PID30 and remain through PID60 [21, 24]. Therefore, the observed circuit reorganization in terms of neuronal hypertrophy (DG, CA3) and dendritic pruning (CA1) may be indicative of an adaptive or reparative process, which facilitates long-term cognitive function. However, long-term performance on sensorimotor, balance, coordination, and turn bias tasks remain significantly impaired through PID60 [24], suggesting that the juvenile brain cannot compensate for all neuropathology resulting from brain injury. In contrast, severe diffuse brain injury in the juvenile induced lasting cognitive deficits [26] and acute pathology that resolved rapidly [27]. Late-onset and long-lasting functional deficits may result from maladaptive or inappropriate circuit reorganization.

No definitive studies can explain the differential responses in CCI-injured PND7 compared to PND17 rats; however, trauma-induced apoptotic neurodegeneration has been found to be enhanced in the DG of PND3 and PND7 rats in comparison to PND10, PND14, and PND30 after the weight drop model of diffuse brain injury [28]. Bittigau et al. suggest that the degree of myelination, brain water content, N-methyl-D-aspartate (NMDA) receptor hypersensitivity period in PND3 and PND7 neonates may leave them more vulnerable to mechanical and excitotoxic injury [43, 44]. Progressive axonal injury and secondary post-injury sequelae may also promote neuron apoptosis in PND3 and PND7 rats due to a combination of excitotoxic neurochemical exposure, circulation of pre-apoptotic molecules and a loss of trophic support due to a loss of afferents [45]. Simply, the younger animals can endure cell death associated with normal development, and the additional pathology from brain injury does not saturate these undefined coping mechanisms. Alternatively, neurons injured directly at PND7 may die, without consequence to surviving neurons, whereas neurons injured at PND17 survive but suffer altered morphology.

Summary

Quantifiable morphological changes occurred in PND17 and PND7 animals at PID28 following CCI, including increased soma area in the DG and CA3 and decreased dendritic length and branching points in CA1. The most robust response was

found in CA1, but did not occur in animals injured at PND7, indicating an age-at-injury response. This study impacts pediatric neurotrauma research by demonstrating that there are both age-dependent and region-dependent morphological changes that result from CCI in juvenile rats. A clear understanding of the chronic structural consequences of brain injury can more completely inform and direct pediatric neurotrauma clinicians and researchers in their approach to improve care, treatment, and rehabilitation.

Acknowledgments The authors would like to sincerely thank the contributions of Dan Santone for the preliminary studies that made this research possible. Also, Rachel K. Rowe, PhD, Jordan L. Harrison, Jenna M. Ziebell, PhD, and the rest of the Translational Neurotrauma Research Team–Phoenix, AZ, provided thoughtful feedback on early drafts of the manuscript. These experiments were carried out at the University of Pittsburgh and analyzed and prepared for publication at the University of Arizona College of Medicine–Phoenix. This work was supported by the Walter L. Copeland Fund of the Pittsburgh Foundation Funding for Cranial Research and Phoenix Children's Hospital Mission Support Funds.

Conflict of interest The authors would like to disclose that there exist no conflicts of interest.

References

1. Faul M, Xu L, Wald MM, Coronado V, Dellinger AM (2010) Traumatic brain injury in the United States: national estimates of prevalence and incidence, 2002-2006. Injury Prev 16:A268
2. Kraus JF, Fife D, Conroy C (1987) Pediatric brain injuries: the nature, clinical course, and early outcomes in a defined United States population. Pediatrics 79:501–507
3. Ewing-Cobbs L, Levin HS, Fletcher JM, Miner ME, Eisenberg HM (1990) The Children's Orientation and Amnesia Test: relationship to severity of acute head injury and to recovery of memory. Neurosurgery 27:683–691
4. Fletcher JM, Ewing-Cobbs L, Francis DJ, Levin HS (1995) Variability in outcomes after traumatic brain injury in children: a developmental perspective. Oxford University Press, New York
5. Schneier AJ, Shields BJ, Hostetler SG, Xiang H, Smith GA (2006) Incidence of pediatric traumatic brain injury and associated hospital resource utilization in the United States. Pediatrics 118:483–492
6. Bruce DA, Schut L, Buruno LA, Wood JH, Sutton LN (1978) Outcome following severe head injuries in children. J Neurosurg 48:679–688
7. Levin HS, Ewing-Cobbs L (1995) Neurobehavioral outcome of pediatric closed head injury. Oxford Univesity Press, New York
8. Beers SR (1992) Cognitive effects of mild head injury in children and adolescents. Neuropsychol Rev 3:281–320
9. Biagas KV, Grundl PD, Kochanek PM, Schiding JK, Nemoto EM (1992) Posttraumatic hyperemia in immature, mature and aged rats: autoradiographic determination of cerebral blood flow. Soc Neurosci Abstr 18:1088
10. Levin HS, Aldrich EF, Saydjari C, Eisenberg HM, Foulkes MA, Bellefleur M, Luerssen TG, Jane JA, Marmarou A, Marshall LF (1992) Experience of the Traumatic Coma Data Bank. Neurosurgery 31:435–443
11. Levin HS (1985) Outcome after head injury: general considerations and neurobehavioral recovery, Washington, D. C.
12. Luerssen TG, Klauber MR, Marshall LF (1988) Outcome from head injury related to patient's age: a longitudinal prospective study of adult and pediatric head injury. J Neurosurg 68:409–416
13. Chauhan NB, Gatto R, Chauhan MB (2010) Neuroanatomical correlation of behavioral deficits in the CCI model of TBI. J Neurosci Methods 190:1–9
14. Dixon CE, Clifton GL, Lighthall JW, Yaghmai AA, Hayes RL (1991) A controlled cortical impact model of traumatic brain injury in the rat. J Neurosci Methods 39:253–262
15. Cherian L, Robertson CS, Contant CF Jr, Bryan RM Jr (1994) Lateral cortical impact injury in rats: cerebrovascular effects of varying depth of cortical deformation and impact velocity. J Neurotrauma 11:573–585
16. Donat CK, Schuhmann MU, Voigt C, Nieber K, Schliebs R, Brust P (2007) Alterations of acetylcholinesterase activity after traumatic brain injury in rats. Brain Inj: [BI] 21:1031–1037
17. Whalen MJ, Dalkara T, You Z, Qiu J, Bermpohl D, Mehta N, Suter B, Bhide PG, Lo EH, Ericsson M, Moskowitz MA (2008) Acute plasmalemma permeability and protracted clearance of injured cells after controlled cortical impact in mice. J Cereb Blood Flow and Metab : Off J Int Soc Cereb Blood Flow and Metab 28:490–505
18. Clark RS, Vagni VA, Nathaniel PD, Jenkins LW, Dixon CE, Szabo C (2007) Local administration of the poly(ADP-ribose) polymerase inhibitor INO-1001 prevents NAD+depletion and improves water maze performance after traumatic brain injury in mice. J Neurotrauma 24:1399–1405
19. Wagner AK, Postal BA, Darrah SD, Chen X, Khan AS (2007) Deficits in novelty exploration after controlled cortical impact. J Neurotrauma 24:1308–1320
20. You Z, Yang J, Takahashi K, Yager PH, Kim HH, Qin T, Stahl GL, Ezekowitz RA, Carroll MC, Whalen MJ (2007) Reduced tissue damage and improved recovery of motor function after traumatic brain injury in mice deficient in complement component C4. J Cereb Blood Flow and Metab: Off J Int Soc Cereb Blood Flow and Metab 27:1954–1964
21. Adelson PD, Fellows-Mayle W, Kochanek PM, Dixon CE (2013) Morris water maze function and histologic characterization of two age-at-injury experimental models of controlled cortical impact in the immature rat. Child's Nerv Syst : ChNS : Off J Int Soc Pediatr Neurosurg 29:43–53
22. Prins ML, Hovda DA (2003) Developing experimental models to address traumatic brain injury in children. J Neurotrauma 20:123–137
23. Stevenson KL, Skinner JC, Davis DS, Tran MP, Dixon PM, Kohanek PM, Jenkins LW, Adeslon PD (2000) Behavioral dysfunction in immature rats after controlled cortical impact. J Neurotrauma 17: 997
24. Ajao DO, Pop V, Kamper JE, Adami A, Rudobeck E, Huang L, Vlkolinsky R, Hartman RE, Ashwal S, Obenaus A, Badaut J (2012) Traumatic brain injury in young rats leads to progressive behavioral deficits coincident with altered tissue properties in adulthood. J Neurotrauma 29:2060–2074
25. Card JP, Santone DJ, Gluhovsky MY, Adelson PD (2005) Plastic reorganization of hippocampal and neocortical circuitry in experimental traumatic brain injury in the immature rat. J Neurotrauma 22: 989–1002
26. Adelson PD, Dixon CE, Kochanek PM (2000) Long-term dysfunction following diffuse traumatic brain injury in the immature rat. J Neurotrauma 17:273–282
27. Adelson PD, Jenkins LW, Hamilton RL, Robichaud P, Tran MP, Kochanek PM (2001) Histopathologic response of the immature rat to diffuse traumatic brain injury. J Neurotrauma 18:967–976
28. Bittigau P, Sifringer M, Pohl D, Stadthaus D, Ishimaru M, Shimizu H, Ikeda M, Lang D, Speer A, Olney JW, Ikonomidou C (1999)

Apoptotic neurodegeneration following trauma is markedly enhanced in the immature brain. Ann Neurol 45:724–735
29. Pohl D, Bittigau P, Ishimaru MJ, Stadthaus D, Hubner C, Olney JW, Turski L, Ikonomidou C (1999) N-Methyl-D-aspartate antagonists and apoptotic cell death triggered by head trauma in developing rat brain. Proc Natl Acad Sci U S A 96:2508–2513
30. Gobbel GT, Bonfield C, Carson-Walter EB, Adelson PD (2007) Diffuse alterations in synaptic protein expression following focal traumatic brain injury in the immature rat. Child's Nerv Syst : ChNS : Off J Int Soc Pediatr Neurosurg 23:1171–1179
31. Adelson PD, Whalen MJ, Kochanek PM, Robichaud P, Carlos TM (1998) Blood brain barrier permeability and acute inflammation in two models of traumatic brain injury in the immature rat: a preliminary report. Acta Neurochirurgica Suppl 71:104–106
32. Scheibel ME, Scheibel AB (1978) The methods of Golgi. Academic, New York, pp 89–114
33. Scheibel ME, Crandall PH, Scheibel AB (1974) The hippocampal-dentate complex in temporal lobe epilepsy. A Golgi Study Epilepsia 15:55–80
34. Card JP, Santone DJ, Vanino DL, Adelson PD (2005) Cytoarchitecture of the neocortex and hippocampus following experimental traumatic brain injury in the immature rat. J Neurotrauma 22:1209
35. Iacono D, O'Brien R, Resnick SM, Zonderman AB, Pletnikova O, Rudow G, An Y, West MJ, Crain B, Troncoso JC (2008) Neuronal hypertrophy in asymptomatic Alzheimer disease. J Neuropathol Exp Neurol 67:578–589
36. Bothwell S, Meredith GE, Phillips J, Staunton H, Doherty C, Grigorenko E, Glazier S, Deadwyler SA, O'Donovan CA, Farrell M (2001) Neuronal hypertrophy in the neocortex of patients with temporal lobe epilepsy. J Neurosci 21:4789–4800
37. Mao H, Elkin BS, Genthikatti VV, Morrison Iii B, 3rd, Yang KH (2013) Why is CA3 more vulnerable than CA1 in experimental models of controlled cortical impact-induced brain injury? J Neurotrauma
38. Anderson KJ, Miller KM, Fugaccia I, Scheff SW (2005) Regional distribution of fluoro-jade B staining in the hippocampus following traumatic brain injury. Exp Neurol 193:125–130
39. Colicos MA, Dixon CE, Dash PK (1996) Delayed, selective neuronal death following experimental cortical impact injury in rats: possible role in memory deficits. Brain Res 739:111–119
40. Kim BT, Rao VL, Sailor KA, Bowen KK, Dempsey RJ (2001) Protective effects of glial cell line-derived neurotrophic factor on hippocampal neurons after traumatic brain injury in rats. J Neurosurg 95:674–679
41. Scheff SW, Price DA, Hicks RR, Baldwin SA, Robinson S, Brackney C (2005) Synaptogenesis in the hippocampal CA1 field following traumatic brain injury. J Neurotrauma 22:719–732
42. Varma MR, Dixon CE, Jackson EK, Peters GW, Melick JA, Griffith RP, Vagni VA, Clark RS, Jenkins LW, Kochanek PM (2002) Administration of adenosine receptor agonists or antagonists after controlled cortical impact in mice: effects on function and histopathology. Brain Res 951:191–201
43. McDonald JW, Silverstein FS, Johnston MV (1988) Neurotoxicity of N-methyl-D-aspartate is markedly enhanced in developing rat central nervous system. Brain Res 459:200–203
44. Ikonomidou C, Mosinger JL, Salles KS, Labruyere J, Olney JW (1989) Sensitivity of the developing rat brain to hypobaric/ischemic damage parallels sensitivity to N-methyl-aspartate neurotoxicity. J Neurosci 9:2809–2818
45. Maxwell WL, Povlishock JT, Graham DL (1997) A mechanistic analysis of nondisruptive axonal injury: a review. J Neurotrauma 14:419–440